ACS OMEGA

http://pubs.acs.org/journal/acsodf

Article

Molecular Dynamics Simulation of a Single Carbon Chain through an Asymmetric Double-Layer Graphene Nanopore for Prolonging the Translocation Time

Yaohong Zhou and Haidong Wang*

Cite This: *ACS Omega* 2022, 7, 16422−16429

Read Online

ACCESS | Metrics & More | Article Recommendations

ABSTRACT: In recent years, sensing technology based on nanopores has become one of the trustworthy options for characterization and even identification of a single biomolecule. In nanopore based DNA sequencing technology, the DNA strand in the electrolyte solution passes through the nanopore under an applied bias electric field. Commonly, the ionic current signals carrying the sequence information are difficult to detect effectively due to the fast translocation speed of the DNA strand, so that slowing down the translocation speed is expected to make the signals easier to distinguish and improve the sequencing accuracy. Modifying the nanopore structure is one of the effective methods. Through all-atom molecular dynamics simulations, we designed an asymmetric double-layer graphene nanopore structure to regulate the translocation speed of a single carbon chain. The structure consists of two nanopores with different sizes located on two layers. The simulation results indicate that the asymmetric nanopore structure will affect the chain's translocation speed and the ionic current value. When the single carbon chain passes from the smaller pore to the larger pore, the translocation time is significantly prolonged, which is about three times as long as the chain passing from the larger pore to the smaller pore. These results provide a new idea for designing more accurate and effective single-molecule solid-state nanopore sensors.

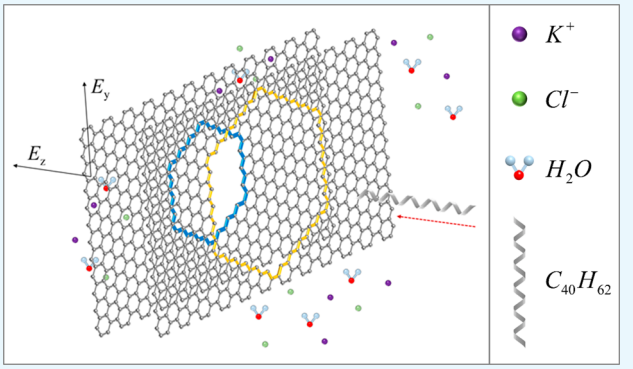

1. INTRODUCTION

Nanopore technology has emerged as a significant research tool for single-molecule analysis and detection.[1−3] One of the most prominent applications is DNA sequencing.[4] This technology typically[5,6] involves applying an applied bias electric field to the electrolyte surrounding the nanopore. A single DNA strand and ions are electrophoretically driven by the electric field. The ordered ion transportation will form a relatively stable ionic current. When the DNA strand passes through the nanopore, it will block the transport of ions. The four kinds of bases in DNA are different in structure, so the blocking effect of each base on ions is different,[7] resulting in different ionic current signals. The sequence information can be read by monitoring the signals of the ionic current during the whole process of DNA passing through the nanopore. The continuous development of this technology is conducive to finally realizing the real-time, high-throughput, and low-cost sequencing of DNA.[8−10] Nanopore technology can be divided into biological nanopore technology and solid-state nanopore technology according to different nanopore materials,[11] among which the biological nanopore membrane usually has a larger thickness (about dozens of nanometers), much larger than the distance between adjacent bases in the DNA strand (only about 0.3−0.5 nm).[12] As a result, it is difficult to distinguish a single base directly. The solid-state nanopore has superior mechanical strength and chemical stability, especially monolayer graphene which has a thickness of 0.334 nm, close to the distance between adjacent bases in the DNA strand. The graphene nanopore is expected to have a higher spatial sensing resolution than the biological nanopore, which becomes a better choice for direct discrimination of a single DNA base;[13] but on the other hand, one of the biggest challenges in real applications of the graphene nanopore[13,14] is that the DNA strand passes through the nanopore very fast due to its atomic thickness, often at an average rate of more than one nucleotide per microsecond. It is too fast to clearly distinguish the four

Received: January 21, 2022
Accepted: April 13, 2022
Published: May 6, 2022

bases of a single DNA strand by monitoring the ionic current signal.[15,16]

Consequently, slowing down the translocation speed has become one of the urgent problems to overcome in order to further improve the sensing accuracy and reliability of a solid-state nanopore. A series of methods have been tried to reduce and control the translocation speed, such as controlling solvent viscosity,[17] increasing contact friction,[18] modifying nanopore structure,[19−25] modifying DNA chain,[26] controlling electric field,[27] etc. If we focus on the idea of regulating the translocation by modifying the nanopore structure, it usually includes physical and chemical modification methods, such as changing the size and shape of the nanopore,[28] chemical functionalization,[29] or surface charge modification.[30] General methods of physical structure modification can prolong the translocation time by increasing the thickness of nanopores,[31] for example, using multilayer nanopore structures. A special kind of multilayer nanopore structure is geometrically asymmetric. Asymmetric nanopore structures are different in shapes, and a conical nanopore is one of the typical asymmetric structures. The influence mechanism of this common asymmetric structure on the translocation process of the DNA chain has been reflected in both experimental[32,33] and simulation studies.[34,35] However, the conical nanopores mentioned in these studies are usually thick. However, increasing the nanopore thickness will also reduce the spatial resolution of single-molecule detection technology, which is not the best solution. Therefore, we proposed an asymmetric double-layer nanopore structure, which can effectively prolong the translocation time and improve the detection accuracy by using a double-layer graphene, maintaining the high spatial resolution of the solid-state nanopore sensor.

In this work, we proposed a new asymmetric double-layer graphene nanopore structure and carried out extensive all-atom molecular dynamics simulations to calculate the translocation time of a single carbon chain passing through the nanopore structure and the corresponding ionic current. The asymmetric nanopore structure consists of two nanopores of different sizes. The larger pore is named the L-pore, and the energy barrier when the single carbon chain passes through the L-pore first is smaller than that when it passes through the smaller pore first, which is conducive to the translocation event of the single carbon chain. The smaller pore is named the S-pore, and the translocation time can be regulated by changing the diameter of the S-pore. Furthermore, the orientation of the single carbon chain passing through the nanopore structure is changed by switching the positions of these two nanopores, and then the effects of the orientation of the single carbon chain passing through the asymmetric nanopore structure on translocation properties and ion transport were revealed. Based on the simulation results, we found that the translocation time of a single carbon chain passing the nanopore from the S-pore to the L-pore can be significantly prolonged and benefit the characterization of molecular structure. This provides an idea for the optimal design and preparation of the solid-state nanopore structure for a longer molecule detection time and higher DNA sequencing accuracy.

2. COMPUTATIONAL METHODS

2.1. System Setup. Figure 1 depicts a schematic of the molecular dynamics simulation model. A box of the KCl solution is divided into cis and trans parts by inserting a membrane of an asymmetric double-layer graphene nanopore

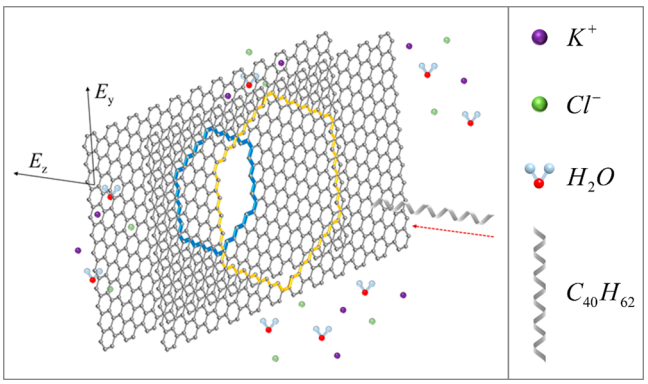

Figure 1. Schematic diagram of the simulation model for a single carbon chain passing through an asymmetric double-layer graphene nanopore.

structure. The box size is 50 × 50 × 102 Å along the *x*, *y*, and *z* directions. Periodic boundary conditions are applied along all three axis directions. The simulation domain contains 2000 water molecules and 300 KCl molecules to keep the KCl concentration at about 2.0 mol/L. The ionic solution environment was kept the same for all the simulation cases, and the influence of the ionic solution environment on the translocation of the carbon chain through the nanopore was consistent in all cases. Two graphene nanopores with different diameters were obtained by removing different numbers of carbon atoms from the centers of two graphene layers. In recent years, there have also been simulation studies using Langevin Molecular Dynamics,[36−38] Monte Carlo,[39−41] and other methods to simulate the translocation process of polymers through a nanopore structure. In these studies, the polymeric chain is just like the DNA strand in nanopore sequencing technology, and the influence of the chain length and pore size on the translocation time has been revealed. In this work, the carbon chain can be seen as the basic skeleton of a DNA molecule.[42] In order to simplify the model, a single carbon chain was used to replace the real DNA strand. The chain is made up of 10 butadiene molecules. The molecular dynamics simulation package LAMMPS[43,44] was adopted to simulate the translocation of a single carbon chain across the asymmetric double-layer graphene nanopores. The reactive force field (ReaxFF[45]) was utilized to describe the interaction between C, H, O, K, and Cl atoms in the simulation.

2.2. ReaxFF Reactive Force Field Method and Data Analysis. In recent years, the development of the reactive force field has made molecular dynamics simulation more practical, and complex hydrocarbon reactions can be better simulated[46] with ReaxFF. New reactive force field[45] parameters have been trained against quantum mechanical (QM) calculations related to water binding energies, hydration energies, and energies of proton transfer, which is suitable for water and electrolyte systems. The water (H/O) parameters have been widely used in various systems, including proteins,[47,48] metal oxides,[49−51] and organic molecules.[52] It can describe the interaction between water molecules and ions such as K^+ and Cl^-. Therefore, this reactive force field can be well applied to our simulated system. The LAMMPS software package was performed to simulate the trajectories of all atoms with the time step of 0.1 fs. First, the conjugate gradient (CG) algorithm was used to minimize the energy of the simulated system. Then, the simulated system was relaxed under the

https://doi.org/10.1021/acsomega.2c00438
ACS Omega 2022, 7, 16422−16429

NPT ensemble for 50 ps to maintain a constant temperature of 300 K and control the pressure to 1 atm. After the relaxation process, the double-layer graphene membrane was fixed in the middle of the simulated system, and the external electric field was applied in the Z-direction (E_z) and Y-direction (E_y), respectively, which covered the entire box. Then, the simulated system ran for 250 ps under the NVT ensemble. In order to improve the efficiency of computation, each carbon atom in the single carbon chain was given a positive charge of one unit. This is similar to negatively charged DNA molecule,[53] which is more visibly affected by electric fields. The cation and anion will move under the application of the electric field. The ionic current can be calculated from the simulated atomic trajectories.

The position coordinates of all atoms in the simulated system were recorded every femtosecond. The ionic current was computed[54] as

$$I(t) = \frac{1}{\Delta t L_z} \sum_{i=1}^{N} q_i[z_i(t + \Delta t) - z_i(t)]$$

where z_i and q_i are the z coordinate and the charge of atom i, respectively. Here, Δt is set to 1 fs, and L_z is the length of the simulated system in the z direction. Furthermore, the ionic current calculated by the above equation was the average value of the instantaneous ionic current during the Δt.

3. RESULTS AND DISCUSSION

3.1. From the L-Pore to the S-Pore. We have made asymmetric nanopores in two graphene layers; the larger pore is named L-pore, while the smaller pore is named S-pore. In the case of the translocation from the L-pore to the S-pore, Table 1 summarizes the translocation status of the single carbon chain when changing the diameter of the S-pore ($D_{S\text{-pore}}$) under different electric field intensities. Figure 2 shows the simulation model and the translocation process when the single carbon chain passes through the L-pore first. The diameter of the L-pore ($D_{L\text{-pore}}$) was fixed at 3.6 nm. Eight groups of S-pores of different sizes were set up, with diameters of 2.0, 2.2, 2.4, 2.6, 2.8, 3.0, 3.2, and 3.4 nm, respectively.

Table 1. Translocation of the Single Carbon Chain while Changing the Diameter of the S-Pore under Different *Z*-Direction and *Y*-Direction Electric Field Intensities

$D_{L\text{-pore}}$ (nm)	$D_{S\text{-pore}}$ (nm)	E_z (V/Å)	E_y (V/Å)	translocation occurred
3.6	2.0	0.15	0.1	yes
3.6	2.2	0.15	0.1	yes
3.6	2.4	0.08	0.05	no
3.6	2.6	0.05	0.05	no
3.6	2.8	0.03	0.05	no
3.6	3.0	0.1	0.05	yes
3.6	3.2	0.1	0.05	yes
3.6	3.4	0.1	0.05	yes
3.6	3.6	0.1	0.05	yes

As shown in Table 1, when the diameter of the L-pore is constant, the smaller the diameter of the S-pore is, and the greater the electric field intensity is required to drive the translocation of the single carbon chain, especially in the Z-direction. It means that a larger barrier needs to be overcome for the single carbon chain to pass through the nanopores. The effect of the pore diameter on the energy barrier is consistent with other computational and experimental studies.[55−57] The value of E_z largely determines the driving force of the single carbon chain; if E_z is not large enough to overcome the resistance in the simulated system, it is difficult for the single carbon chain to pass through the nanopores. The resistance consists of liquid viscosity resistance, interaction between the the single carbon chain and graphene nanopores, and charge repulsion.[58] It is worth noting that the application of the Y-direction electric field can effectively bring the single carbon chain closer to the position of the nanopores. Simulation results show that without the application of the Y-direction electric field, the single carbon chain is easily adsorbed on the surface of graphene, which means that it is difficult for the chain to pass through the nanopore.

Under the same electric field parameters, with different diameters of the S-pore, the duration of the single carbon chain passing through the nanopores is different; as shown in Figure 3(a), the duration decreases nonlinearly as the diameter of the S-pore increases linearly. This indicates that for the two nanopores in the simulated system, the regulation of the duration can be realized by only changing the diameter of one of the nanopores, and the duration is sensitive to the change of pore diameter. However, this feedback is not significantly reflected in the simulation results of the ionic current. As shown in Figure 3(b), under the same electric field parameters, the smaller the diameter of the S-pore is, the smaller the overall level of the ionic current is; but the difference between ionic currents is not significant, because the diameter of the S-pore does not change much. In addition, the variation trend of the simulated ionic current is similar to that in ref 58. That is, after the electric field is applied, the ionic current will step up to a maximum value and then drop to a relatively stable value, which may also include the blocking value caused by the volume occupying effect[59] of the single carbon chain. The ionic current in Figure 3(b) was calculated at the moment when the electric field was applied.

3.2. From the S-Pore to the L-Pore. In the case of the translocation from the S-pore to the L-pore, the single carbon chain can pass through the asymmetric double-layer nanopore when E_z = 0.1 V/Å and E_y = 0.05 V/Å, regardless of the S-pore's diameter, as shown in Table 2. It suggests that the electric field restriction is less stringent when passing through the nanopore from the S-pore to the L-pore than that in the opposite direction. Here, the diameter of the L-pore was also fixed as 3.6 nm. The atomic trajectory results obtained by the simulation indicate that, when the single carbon chain passes through the L-pore first (as shown in Figure 2), the ion flux is larger, so the space near the S-pore will accumulate K^+ faster, and the space near the L-pore will accumulate Cl^- faster. As a result, the single carbon chain will be constrained by the greater resistance. When the S-pore is not large enough, it is difficult for the single carbon chain to complete the translocation due to the excessive resistance. However, if the chain passes through the S-pore first (as shown in Figure 4), the ion flux will decrease, which helps to reduce resistance caused by ion accumulation. This makes it easier for the carbon chain to pass through. Figure 5 compares the duration of the translocation of a single molecule in two cases.

As shown in Figure 5, it is obvious that when the single carbon chain passes through the S-pore first, the duration of the translocation is longer. The effect of the S-pore's diameter on the duration is similar to that of passing through the L-pore

https://doi.org/10.1021/acsomega.2c00438
ACS Omega 2022, 7, 16422−16429

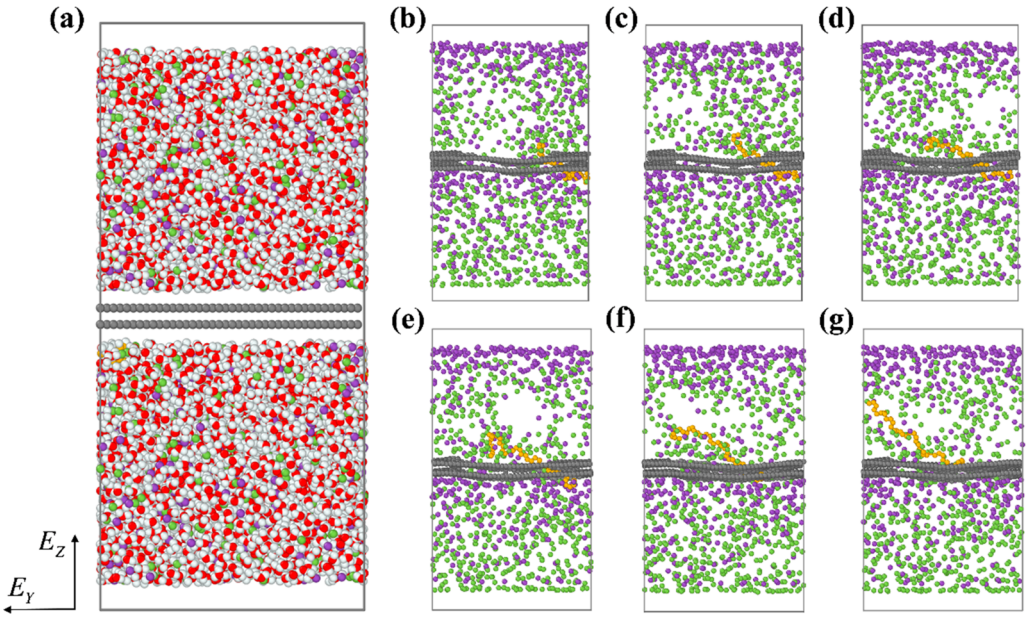

Figure 2. Molecular dynamics simulation of the single carbon chain passing through the L-S type nanopore structure under an applied bias electric field. (a) The simulation model: the single carbon chain is shown in yellow, other carbon atoms are shown in gray, the hydrogen atoms are shown in white, the oxygen atoms are shown in red, the potassium ions are shown in purple, and the chloride ions are shown in green. (b)−(g) together demonstrate the translocation process of the single carbon chain passing through the nanopore structure.

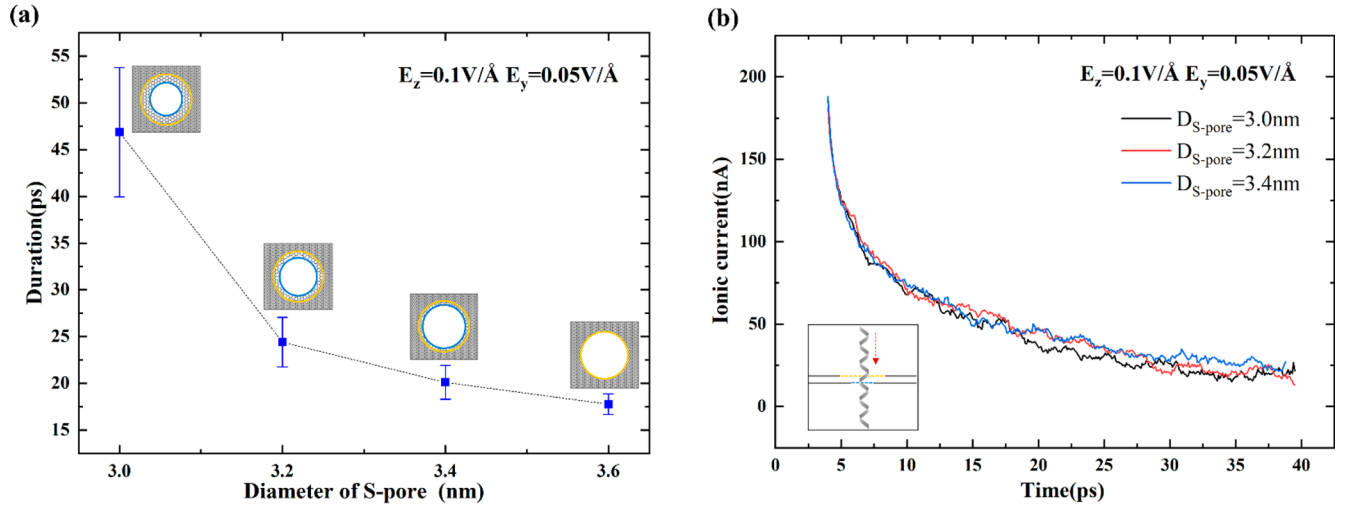

Figure 3. (a) The duration for the translocation of the single carbon chain when the diameter of the S-pore is 3.0, 3.2, 3.4, and 3.6 nm, E_z = 0.1 V/Å, and E_y = 0.05 V/Å. (b) The ionic current during the translocation of the single carbon chain when the diameter of the S-pore is 3.0, 3.2, and 3.4 nm, E_z= 0.1 V/Å, and E_y = 0.05 V/Å.

Table 2. Translocation of the Single Carbon Chain while Changing the Diameter of the S-Pore at E_z = 0.1 V/Å and E_y = 0.05 V/Å

$D_{S\text{-}pore}$ (nm)	$D_{L\text{-}pore}$ (nm)	E_z (V/Å)	E_y (V/Å)	translocation occurred
2.0	3.6	0.1	0.05	yes
2.2	3.6	0.1	0.05	yes
2.4	3.6	0.1	0.05	yes
2.6	3.6	0.1	0.05	yes
2.8	3.6	0.1	0.05	yes
3.0	3.6	0.1	0.05	yes
3.2	3.6	0.1	0.05	yes

first. This suggests that the duration can be regulated by controlling the diameter of the S-pore in both cases. Moreover, the case of passing through the S-pore first can better prolong the duration time, which is about three times as long as that passing through the L-pore first. In this case, the S-pore can also reduce ion flux and help the single carbon chain to better complete the translocation. However, the reduction of the ion flux also brings some problems. When the single carbon chain passes through the nanopores, the ion transport will be blocked, reflecting the volume occupying effect.[60,61] As the ion flux is lower if passing through the S-pore first, the volume occupying effect will be weakened. This will also result in a smaller overall level of the ionic current. Figure 6(a) shows the ionic current calculation results when the diameter of the S-pore is 2.2, 2.4, 2.6, 2.8, 3.0, and 3.2 nm, respectively, E_z = 0.1 V/Å, and E_y = 0.05 V/Å. Figure 6(b) shows the ionic current when the single carbon chain in the system is removed.

https://doi.org/10.1021/acsomega.2c00438
ACS Omega 2022, 7, 16422−16429

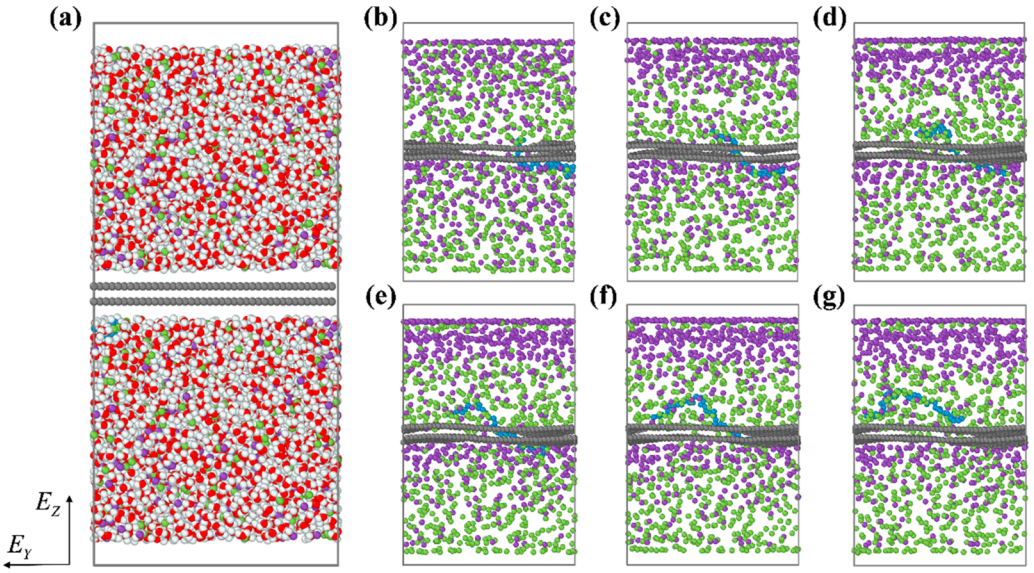

Figure 4. Molecular dynamics simulation of the single carbon chain passing through the S-L type nanopore structure under an applied bias electric field. (a) The simulation model: the single carbon chain is shown in blue, other carbon atoms are shown in gray, the hydrogen atoms are shown in white, the oxygen atoms are shown in red, the potassium ions are shown in purple, and the chloride ions are shown in green. (b)−(g) together demonstrate the translocation process of the single carbon chain passing through the nanopore structure.

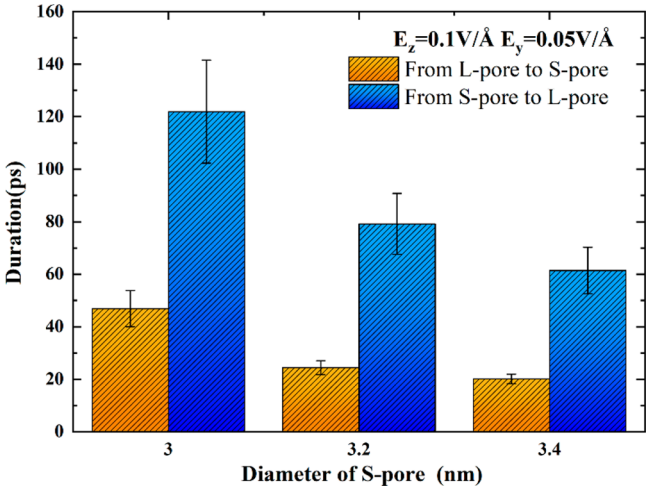

Figure 5. Comparison of the translocation duration in two cases, where the diameter of the S-pore is 3.0, 3.2, and 3.4 nm, E_z = 0.1 V/Å, and E_y = 0.05 V/Å.

Comparing the ionic current results in Figure 6(a) and Figure 6(b), the blocking effect of the single carbon chain on the ionic current will be clearly revealed. Figure 6(c) and Figure 6(d) show the ionic current blocking of the single carbon chain passing through the nanopores in two cases (in two opposite directions) when the S-pore's diameter is 3.0 nm.

Figure 6(a) and Figure 6(b) suggest that, regardless of whether there is a single carbon chain in the simulated system, the larger the S-pore's diameter is, the larger the overall level of the ionic current is. The ionic current decreases with the decrease of the S-pore's diameter.[62] However, if comparing Figure 6(a) and Figure 6(b), it can be seen that when the single carbon chain is removed, the volume occupying effect disappears, which leads to the increase of the ion flux, so the ionic current drops faster, which shows up as a steeper curve in Figure 6(b). Similar to the results mentioned above, due to the small difference in the S-pore's diameter, there is no obvious difference in the calculated ionic current, but the difference still can be seen. Figure 6(c) shows the current blockage phenomenon caused by the volume occupying effect in the case of passing through the S-pore first. Compare the results as shown in Figure 6(d). The current blockage is weaker than the case of passing through the L-pore first. This indicates that the S-pore's diameter constrains the ion flux, and the smaller the ion flux is limited, the weaker the current blockage phenomenon will become. It means that when the single carbon chain passes in the direction from the S-pore to the L-pore, the resistance of ion accumulation will be reduced, and the volume occupying effect is weakened; but it is worth noting that the translocation event can still be detected even though the volume occupying effect is weakened.

4. CONCLUSIONS

In this work, molecular dynamics simulation was used to study the translocation properties of the single carbon chain in two types of asymmetric double-layer graphene nanopores. The incidence of translocation events based on S-L type nanopores (from the S-pore to the L-pore) was better than that based on L-S type nanopores (from the L-pore to the S-pore). The translocation of the single charged carbon chain is affected by the accumulation of ions on either side of the nanopores. In the case of L-S type nanopores, if the translocation of the chain is still not completed until the ion concentration reaches a high level, it will be difficult for the chain to pass through the nanopore due to the higher charge repulsion attribute to the faster ion accumulation; but the S-L type nanopore structure can reduce the ion flux, thus slowing down the ion accumulation rate, which is beneficial to the translocation. Regardless of the L-S or S-L type nanopore structure, the duration of the single carbon chain passing through the nanopore can be regulated by only controlling the size of the nanopore in one layer of the graphene membrane. The duration obtained by using the S-L type nanopore structure is about three times as long as that of the L-S type nanopore structure. It has a good inspiration for improving the single-

https://doi.org/10.1021/acsomega.2c00438
ACS Omega 2022, 7, 16422−16429

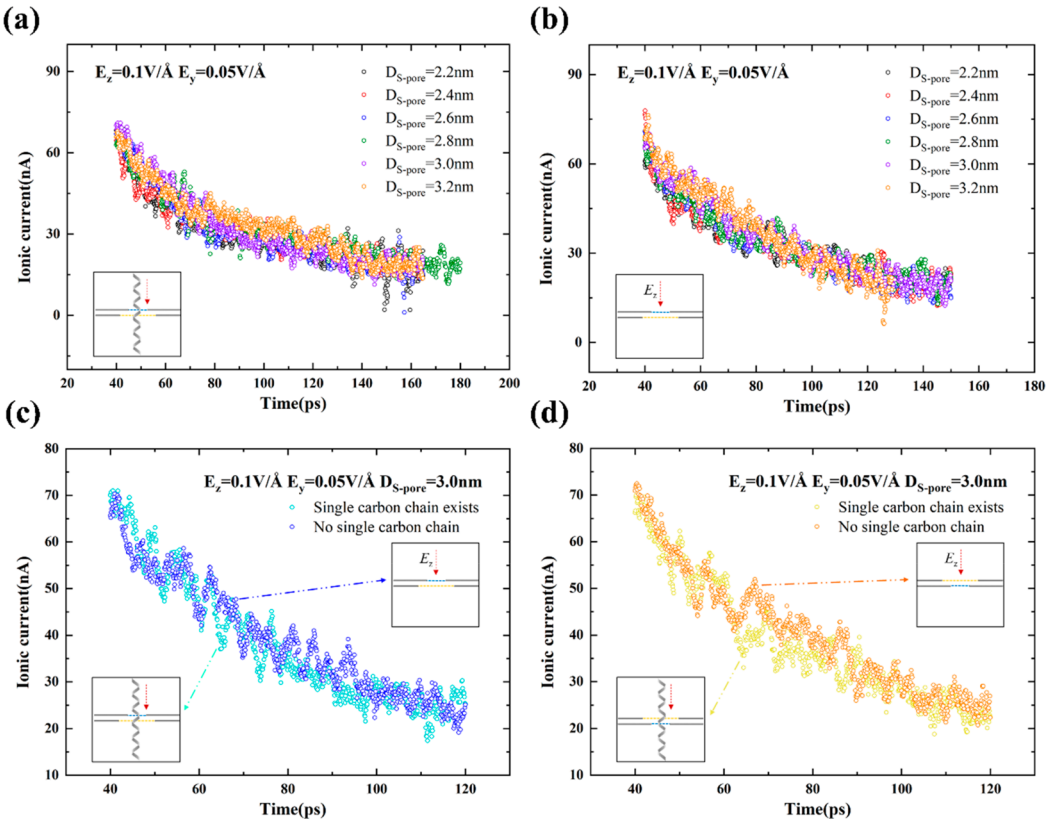

Figure 6. Ionic current of the single carbon chain passing through double-layer graphene. (a) When the single carbon chain existed in the simulated system. The ionic current calculation results when the diameter of the S-pore is 2.2, 2.4, 2.6, 2.8, 3.0, and 3.2 nm, respectively, E_z = 0.1 V/Å, and E_y = 0.05 V/Å. (b) When the single carbon chain was removed. The ionic current calculation results when the diameter of the S-pore is 2.2, 2.4, 2.6, 2.8, 3.0, and 3.2 nm, respectively, E_z = 0.1 V/Å, and E_y = 0.05 V/Å. (c) When the single carbon chain passes through the S-pore first. The calculation results of the ionic current with and without the single carbon chain in the simulated system, when the S-pore's diameter is 3.0 nm, E_z = 0.1 V/Å, and E_y = 0.05 V/Å. (d) When the single carbon chain passes through the L-pore first. The calculation results of the ionic current with and without the single carbon chain in the simulated system, when the S-pore's diameter is 3.0 nm, E_z = 0.1 V/Å, and E_y = 0.05 V/Å.

molecule nanopore detection technology by using the asymmetric nanopore structure. The S-L type nanopore structure is more conducive to reduce the translocation speed, even though the ionic current will be reduced as well. Moreover, the reduced ionic current has limited influence on the identification of a single molecule. The proposed asymmetric nanopore structure and simulation results provide new ideas for the design and preparation of solid-state nanopore structures for prolonging detection time and achieving higher accuracy.

AUTHOR INFORMATION

Corresponding Author

Haidong Wang − *Key Laboratory for Thermal Science and Power Engineering of Ministry of Education, Department of Engineering Mechanics, Tsinghua University, Beijing 100084, China;* orcid.org/0000-0001-8933-2279; Email: hdwang@tsinghua.edu.cn

Author

Yaohong Zhou − *Key Laboratory for Thermal Science and Power Engineering of Ministry of Education, Department of Engineering Mechanics, Tsinghua University, Beijing 100084, China;* orcid.org/0000-0001-7094-3512

Complete contact information is available at: https://pubs.acs.org/10.1021/acsomega.2c00438

Notes

The authors declare no competing financial interest.

ACKNOWLEDGMENTS

This work was supported by the National Natural Science Foundation of China (No. 51976096) and the National Youth 1000 Talents Program in China. The simulation work is based on the parallel computing servers, CPU: Intel Xeon Scalable2 (2.4 GHz), 24 cores*4. A single simulation case can be completed in about 70 h.

REFERENCES

(1) Aksimentiev, A. Deciphering ionic current signatures of DNA transport through a nanopore. *Nanoscale* **2010**, *2* (4), 468−483.
(2) Dekker, C. Solid-state nanopores. *Nanosci. technol.* **2009**, 60−66.
(3) Rodrigues, C. G.; Machado, D. C.; Chevtchenko, S. F.; Krasilnikov, O. V. Mechanism of KCl enhancement in detection of nonionic polymers by nanopore sensors. *Biophys. J.* **2008**, *95* (11), 5186−5192.
(4) Branton, D.; Deamer, D. W.; Marziali, A.; Bayley, H.; Benner, S. A.; Butler, T.; Di Ventra, M.; Garaj, S.; Hibbs, A.; Huang, X. The potential and challenges of nanopore sequencing. *Nanosci. technol.* **2009**, 261−268.
(5) Kasianowicz, J. J. Nanometer-scale pores: potential applications for analyte detection and DNA characterization. *Dis. Markers.* **2002**, *18* (4), 185−191.
(6) Kasianowicz, J. J.; Brandin, E.; Branton, D.; Deamer, D. W. Characterization of individual polynucleotide molecules using a

https://doi.org/10.1021/acsomega.2c00438
ACS Omega 2022, 7, 16422−16429

membrane channel. *Proc. Natl. Acad. Sci. U. S. A.* **1996**, *93* (24), 13770−13773.
(7) Bayley, H. Nanopore sequencing: from imagination to reality. *Clin. Chem.* **2015**, *61* (1), 25−31.
(8) Pathak, B.; Löfås, H.; Prasongkit, J.; Grigoriev, A.; Ahuja, R.; Scheicher, R. H. Double-functionalized nanopore-embedded gold electrodes for rapid DNA sequencing. *Appl. Phys. Lett.* **2012**, *100* (2), 023701.
(9) Pomerantz, A.; Peñafiel, N.; Arteaga, A.; Bustamante, L.; Pichardo, F.; Coloma, L. A.; Barrio-Amorós, C. L.; Salazar-Valenzuela, D.; Prost, S. Real-time DNA barcoding in a rainforest using nanopore sequencing: opportunities for rapid biodiversity assessments and local capacity building. *GigaScience* **2018**, *7* (4), giy033.
(10) Wei, S.; Weiss, Z. R.; Williams, Z. Rapid multiplex small DNA sequencing on the MinION nanopore sequencing platform. *G3: Genes, Genomes, Genet.* **2018**, *8* (5), 1649−1657.
(11) Deng, T.; Li, M.; Wang, Y.; Liu, Z. Development of solid-state nanopore fabrication technologies. *Sci. Bull.* **2015**, *60* (3), 304−319.
(12) Pruneanu, S.; Al-Said, S. A. F.; Dong, L.; Hollis, T. A.; Galindo, M. A.; Wright, N. G.; Houlton, A.; Horrocks, B. R. Self-Assembly of DNA-Templated Polypyrrole Nanowires: Spontaneous Formation of Conductive Nanoropes. *Adv. Funct. Mater.* **2008**, *18* (16), 2444−2454.
(13) Siwy, Z. S.; Davenport, M. Graphene opens up to DNA. *Nat. Nanotechnol.* **2010**, *5* (10), 697−698.
(14) Luan, B.; Stolovitzky, G.; Martyna, G. Slowing and controlling the translocation of DNA in a solid-state nanopore. *Nanoscale* **2012**, *4* (4), 1068−1077.
(15) Huang, S.; He, J.; Chang, S.; Zhang, P.; Liang, F.; Li, S.; Tuchband, M.; Fuhrmann, A.; Ros, R.; Lindsay, S. Identifying single bases in a DNA oligomer with electron tunnelling. *Nat. Nanotechnol.* **2010**, *5* (12), 868−873.
(16) Tsutsui, M.; Taniguchi, M.; Yokota, K.; Kawai, T. Identifying single nucleotides by tunnelling current. *Nat. Nanotechnol.* **2010**, *5* (4), 286−290.
(17) Fologea, D.; Uplinger, J.; Thomas, B.; McNabb, D. S.; Li, J. Slowing DNA translocation in a solid-state nanopore. *Nano Lett.* **2005**, *5* (9), 1734−1737.
(18) Mirsaidov, U.; Comer, J.; Dimitrov, V.; Aksimentiev, A.; Timp, G. Slowing the translocation of double-stranded DNA using a nanopore smaller than the double helix. *Nanotechnology* **2010**, *21* (39), 395501.
(19) Luan, B.; Afzali, A.; Harrer, S.; Peng, H.; Waggoner, P.; Polonsky, S.; Stolovitzky, G.; Martyna, G. Tribological effects on DNA translocation in a nanochannel coated with a self-assembled monolayer. *J. Phys. Chem. B* **2010**, *114* (51), 17172−17176.
(20) Wanunu, M.; Meller, A. Chemically modified solid-state nanopores. *Nano Lett.* **2007**, *7* (6), 1580−1585.
(21) Wei, R.; Gatterdam, V.; Wieneke, R.; Tampé, R.; Rant, U. Stochastic sensing of proteins with receptor-modified solid-state nanopores. *Nat. Nanotechnol.* **2012**, *7* (4), 257−263.
(22) Gyurcsányi, R. E. Chemically-modified nanopores for sensing. *TrAC, Trends Anal. Chem.* **2008**, *27* (7), 627−639.
(23) Miles, B. N.; Ivanov, A. P.; Wilson, K. A.; Doğan, F.; Japrung, D.; Edel, J. B. Single molecule sensing with solid-state nanopores: novel materials, methods, and applications. *Chem. Soc. Rev.* **2013**, *42* (1), 15−28.
(24) Tang, Z.; Lu, B.; Zhao, Q.; Wang, J.; Luo, K.; Yu, D. Surface Modification of Solid-State Nanopores for Sticky-Free Translocation of Single-Stranded DNA. *Small* **2014**, *10* (21), 4332−4339.
(25) Yeh, L.-H.; Zhang, M.; Qian, S.; Hsu, J.-P. Regulating DNA translocation through functionalized soft nanopores. *Nanoscale* **2012**, *4* (8), 2685−2693.
(26) Carlsen, A. T.; Zahid, O. K.; Ruzicka, J. A.; Taylor, E. W.; Hall, A. R. Selective detection and quantification of modified DNA with solid-state nanopores. *Nano Lett.* **2014**, *14* (10), 5488−5492.
(27) Sigalov, G.; Comer, J.; Timp, G.; Aksimentiev, A. Detection of DNA sequences using an alternating electric field in a nanopore capacitor. *Nano Lett.* **2008**, *8* (1), 56−63.
(28) Zou, A.; Xiu, P.; Ou, X.; Zhou, R. Spontaneous translocation of single-stranded DNA in graphene−MoS2 heterostructure nanopores: shape effect. *J. Phys. Chem. B* **2020**, *124* (43), 9490−9496.
(29) Karmi, A.; Sakala, G. P.; Rotem, D.; Reches, M.; Porath, D. Durable, stable, and functional nanopores decorated by self-assembled dipeptides. *ACS Appl. Mater. Interfaces* **2020**, *12* (12), 14563−14568.
(30) Luan, B.; Aksimentiev, A. Control and reversal of the electrophoretic force on DNA in a charged nanopore. *J. Phys.: Condens. Matter* **2010**, *22* (45), 454123.
(31) Si, W.; Sha, J. J.; Liu, L.; Li, J. P.; Wei, X. L.; Chen, Y. F. In *Detecting DNA using a single graphene pore by molecular dynamics simulations*; Key Engineering Materials, Trans Tech Publ: 2012; pp 423−426, DOI: 10.4028/www.scientific.net/KEM.503.423.
(32) Mara, A.; Siwy, Z.; Trautmann, C.; Wan, J.; Kamme, F. An asymmetric polymer nanopore for single molecule detection. *Nano Lett.* **2004**, *4* (3), 497−501.
(33) Harrell, C. C.; Choi, Y.; Horne, L. P.; Baker, L. A.; Siwy, Z. S.; Martin, C. R. Resistive-pulse DNA detection with a conical nanopore sensor. *Langmuir* **2006**, *22* (25), 10837−10843.
(34) Sun, L.-Z.; Li, H.; Xu, X.; Luo, M.-B. Simulation study on the translocation of polyelectrolyte through conical nanopores. *J. Phys.: Condens. Matter* **2018**, *30* (49), 495101.
(35) Domański, Z.; Grzybowski, A. Z. Simulation Study of Chain-like Body Translocation through Conical Pores in Thick Membranes. *Membranes* **2022**, *12* (2), 138.
(36) Forrey, C.; Muthukumar, M. Langevin dynamics simulations of ds-DNA translocation through synthetic nanopores. *J. Chem. Phys.* **2007**, *127* (1), 015102.
(37) Huopaniemi, I.; Luo, K.; Ala-Nissila, T.; Ying, S.-C. Langevin dynamics simulations of polymer translocation through nanopores. *J. Chem. Phys.* **2006**, *125* (12), 124901.
(38) Sun, L.-Z.; Luo, M.-B. Study on the polymer translocation induced blockade ionic current inside a nanopore by Langevin dynamics simulation. *J. Phys.: Condens. Matter* **2013**, *25* (46), 465101.
(39) Luo, K.; Ala-Nissila, T.; Ying, S.-C. Polymer translocation through a nanopore: A two-dimensional Monte Carlo study. *J. Chem. Phys.* **2006**, *124* (3), 034714.
(40) Milchev, A.; Binder, K.; Bhattacharya, A. Polymer translocation through a nanopore induced by adsorption: Monte Carlo simulation of a coarse-grained model. *J. Chem. Phys.* **2004**, *121* (12), 6042−6051.
(41) Gauthier, M. G.; Slater, G. W. A Monte Carlo algorithm to study polymer translocation through nanopores. I. Theory and numerical approach. *J. Chem. Phys.* **2008**, *128* (6), 065103.
(42) Sinden, R. R. *DNA structure and function*; Gulf Professional Publishing: 1994; DOI: 10.1016/C2009-0-02451-9.
(43) Plimpton, S. Fast parallel algorithms for short-range molecular dynamics. *J. Comput. Phys.* **1995**, *117* (1), 1−19.
(44) Aktulga, H. M.; Fogarty, J. C.; Pandit, S. A.; Grama, A. Y. Parallel reactive molecular dynamics: Numerical methods and algorithmic techniques. *Parallel Comput* **2012**, *38* (4−5), 245−259.
(45) Fedkin, M. V.; Shin, Y. K.; Dasgupta, N.; Yeon, J.; Zhang, W.; van Duin, D.; van Duin, A. C. T.; Mori, K.; Fujiwara, A.; Machida, M.; Nakamura, H.; Okumura, M. Development of the ReaxFF Methodology for Electrolyte-Water Systems. *J. Phys. Chem. A* **2019**, *123* (10), 2125−2141.
(46) Van Duin, A. C.; Dasgupta, S.; Lorant, F.; Goddard, W. A. ReaxFF: a reactive force field for hydrocarbons. *J. Phys. Chem. A* **2001**, *105* (41), 9396−9409.
(47) Monti, S.; Corozzi, A.; Fristrup, P.; Joshi, K. L.; Shin, Y. K.; Oelschlaeger, P.; Van Duin, A. C.; Barone, V. Exploring the conformational and reactive dynamics of biomolecules in solution using an extended version of the glycine reactive force field. *Phys. Chem. Chem. Phys.* **2013**, *15* (36), 15062−15077.
(48) Rahaman, O.; Van Duin, A. C.; Goddard, W. A., III; Doren, D. J. Development of a ReaxFF reactive force field for glycine and application to solvent effect and tautomerization. *J. Phys. Chem. B* **2011**, *115* (2), 249−261.

https://doi.org/10.1021/acsomega.2c00438
ACS Omega 2022, 7, 16422−16429

(49) Raymand, D.; van Duin, A. C.; Spångberg, D.; Goddard, W. A., III; Hermansson, K. Water adsorption on stepped ZnO surfaces from MD simulation. *Surf. Sci.* **2010**, *604* (9−10), 741−752.
(50) Shin, Y. K.; Kwak, H.; Vasenkov, A. V.; Sengupta, D.; Van Duin, A. C. Development of a ReaxFF reactive force field for Fe/Cr/O/S and application to oxidation of butane over a pyrite-covered Cr2O3 catalyst. *ACS Catal.* **2015**, *5* (12), 7226−7236.
(51) Van Duin, A. C.; Bryantsev, V. S.; Diallo, M. S.; Goddard, W. A.; Rahaman, O.; Doren, D. J.; Raymand, D.; Hermansson, K. Development and validation of a ReaxFF reactive force field for Cu cation/water interactions and copper metal/metal oxide/metal hydroxide condensed phases. *J. Phys. Chem. A* **2010**, *114* (35), 9507−9514.
(52) Abolfath, R. M.; Van Duin, A.; Brabec, T. Reactive molecular dynamics study on the first steps of DNA damage by free hydroxyl radicals. *J. Phys. Chem. A* **2011**, *115* (40), 11045−11049.
(53) Fritz, J.; Cooper, E. B.; Gaudet, S.; Sorger, P. K.; Manalis, S. R. Electronic detection of DNA by its intrinsic molecular charge. *Proc. Natl. Acad. Sci. U. S. A.* **2002**, *99* (22), 14142−14146.
(54) Aksimentiev, A.; Heng, J. B.; Timp, G.; Schulten, K. Microscopic Kinetics of DNA Translocation through synthetic nanopores. *Biophys. J.* **2004**, *87* (3), 2086−97.
(55) Gai, J.-G.; Gong, X.-L.; Wang, W.-W.; Zhang, X.; Kang, W.-L. An ultrafast water transport forward osmosis membrane: porous graphene. *J. Phys. Chem. A* **2014**, *2* (11), 4023−4028.
(56) Li, J.; Wang, H.; Li, Y.; Han, K. The impact of the number of layers of the graphene nanopores and the electrical field on ssDNA translocation. *Mol. Simul.* **2017**, *43* (4), 320−325.
(57) Suma, A.; Micheletti, C. Pore translocation of knotted DNA rings. *Proc. Natl. Acad. Sci. U. S. A.* **2017**, *114* (15), E2991−E2997.
(58) Li, J.; Zhang, Y.; Yang, J.; Bi, K.; Ni, Z.; Li, D.; Chen, Y. Molecular dynamics study of DNA translocation through graphene nanopores. *Phys. Rev. E: Stat., Nonlinear, Soft Matter Phys.* **2013**, *87* (6), 062707.
(59) Xue, L.; Yamazaki, H.; Ren, R.; Wanunu, M.; Ivanov, A. P.; Edel, J. B. Solid-state nanopore sensors. *Nat. Rev. Mater.* **2020**, *5* (12), 931−951.
(60) Clarke, J.; Wu, H.-C.; Jayasinghe, L.; Patel, A.; Reid, S.; Bayley, H. Continuous base identification for single-molecule nanopore DNA sequencing. *Nat. Nanotechnol.* **2009**, *4* (4), 265−270.
(61) Manrao, E. A.; Derrington, I. M.; Laszlo, A. H.; Langford, K. W.; Hopper, M. K.; Gillgren, N.; Pavlenok, M.; Niederweis, M.; Gundlach, J. H. Reading DNA at single-nucleotide resolution with a mutant MspA nanopore and phi29 DNA polymerase. *Nat. Biotechnol.* **2012**, *30* (4), 349−353.
(62) Bhattacharya, S.; Derrington, I. M.; Pavlenok, M.; Niederweis, M.; Gundlach, J. H.; Aksimentiev, A. Molecular dynamics study of MspA arginine mutants predicts slow DNA translocations and ion current blockades indicative of DNA sequence. *ACS Nano* **2012**, *6* (8), 6960−6968.

https://doi.org/10.1021/acsomega.2c00438
ACS Omega 2022, 7, 16422−16429